JOURNAL OF GUIDANCE, CONTROL, AND DYNAMICS
Vol. 19, No. 6, November–December 1996

First Results of Reduced Dynamics with DORIS on TOPEX/Poseidon and SPOT

Béatrice Barotto* and Jean-Paul Berthias†
Centre National d'Etudes Spatiales, 31401 Toulouse Cedex 4, France

Highly accurate force models have been developed to achieve the very accurate orbit determination required for the French-American oceanographic mission TOPEX/Poseidon. However, these models are still not accurate enough to explain all of the signatures observed in the Doppler orbitography and radiopositioning integrated by satellite (DORIS) and satellite laser ranging residuals. The excellent orbital coverage and the high quality of the data make it possible to evaluate the level of the error in the dynamical models. To extract this information, an improved filter-smoother method has been implemented. It combines a least-squares approach, in the Givens square root formulation, with stochastic parameters. This filter is used to compute the amplitude of an empirical stochastic force. This fictitious force has been evaluated as part of an orbit determination process over several cycles. Its amplitude is at the level of 10^{-9} m/s^2.

Introduction

WITH the advent of new tracking systems, which offer both a high density of measurements and a global coverage of the orbit, it has become common practice to solve for empirical corrections to poorly known dynamical models. These empirical corrections take the form of piecewise constant multiplicative coefficients such as the 6-h drag coefficient or the daily once per revolution terms. These parameters are uncorrelated; that is, the coefficient on the $n + 1$th interval does not depend on the value of the coefficient on the nth interval. These parameters are introduced in the normal single batch least-squares filter as N independent constant parameters, or biases, despite the fact that they actually influence the motion of the spacecraft only during one interval.

A better approach is to consider parameters that are functions of time. In practice, piecewise constants are satisfactory representations for any function, as long as the interval over which they are constant is kept short compared with the characteristic time of the physical effect that is modeled. In opposition to the previously mentioned coefficients, these parameters obey evolution equations of their own and are therefore correlated from one interval to the next.

However, if the evolution equations are deterministic, they can be incorporated in the dynamical model, and the problem is solved. Hence, it is only for the case of parameters that obey stochastic time propagation equations that this formalism is useful. The coefficients are then called stochastic parameters.

Stochastic parameters were first introduced in interplanetary orbit determination to take full advantage of the accurate tracking data despite errors in the dynamical models. Gas leaks were typically modeled as stochastic accelerations and solved for.

This technique was applied to the processing of Seasat S-band Doppler and satellite laser ranging (SLR) data.[1] The drag coefficient was modeled as a stochastic parameter, in addition to stochastic accelerations. The resulting orbit quality improvement was on the order of 30%, limited by the insufficiency and maldistribution of the data.

This technique has been refined and adapted to process the TOPEX/Poseidon Global Positioning System (GPS) tracking data.[2] The reduced dynamics tracking approach to computing orbits relies on the fact that the geometrical information contained in the GPS data in the three directions is almost sufficient to compute the orbit. In this case, the importance of the dynamical models can be significantly reduced. In the Jet Propulsion Laboratory (JPL) "grand" solution, a large number of parameters are therefore stochastic (clock biases, zenith atmospheric delay, empirical accelerations).

Doppler orbitography and radiopositioning integrated by satellite (DORIS) does not offer this possibility of computing the orbit without a dynamical model. Despite remarkable improvements in the dynamical models,[3] the accuracy of the data remains such that models alone are not sufficient. In our reduced dynamics orbit determinations, we do not solve for a coefficient from a force model but rather for the components of an empirical stochastic force acting on the spacecraft. This method relies on the fact that the DORIS measurements determine accelerations more accurately than the current models can model them. Hence, by giving some added weight to the measurements, it is expected that the stochastically corrected orbit will be closer to the actual spacecraft orbit than the classical fully dynamical solution.

In the following sections, this paper presents the filter used to process measurements, followed by a short description of the orbit determination configuration. Results obtained with a few cycles of TOPEX/Poseidon data are presented and discussed. Our first results with SPOT data are also included.

Filter Formulation

Let t_{start} and t_{end} be the beginning and the end of the measurement cycle, respectively. In a classical least-squares problem, all of the measurements performed during this cycle are processed in a single batch. The adjusted parameters are constant over this entire time period.

In the least-squares problem with stochastic parameters, the interval $[t_{\text{start}}, t_{\text{end}}]$ is divided into many subintervals $[t_j, t_{j+1}]$, of length d. Measurements are accordingly divided into small batches. The stochastic parameters are assumed constant over each small interval and are noted p_j. To completely specify the system, a time evolution for the various p must be chosen. We assume that $p(t)$ is a first-order Gauss–Markov random process, which satisfies the first-order differential equation

$$\frac{\mathrm{d}p(t)}{\mathrm{d}t} = -\frac{1}{\tau}\,p(t) + \omega(t)$$

where $\omega(t)$ is a zero mean white noise with variance Q. The term τ is the correlation time of the process. Integration of this equation at discrete times yields a recursive form of the propagation equation

$$p(t_{j+1}) = M(t_{j+1}, t_j)p(t_j) + \eta_j$$

Presented as Paper 94-3778 at the AIAA/AAS Astrodynamics Conference, Scottsdale, AZ, Aug. 1–3, 1994; received Sept. 24, 1994; revision received Sept. 12, 1995; accepted for publication March 18, 1996.

*Doctoral Fellow, Division Mathématiques Spatiales, Département Métrologie et Techniques Orbitales, and Laboratoire de Mathématiques pour l'Industrie et la Physique, Université Paul Sabatier, 118 route de Narbonne, 31062 Toulouse Cedex.

†Member, Technical Staff, Division Mathématiques Spatiales, Département Métrologie et Techniques Orbitales, BPi 1214.

where

$$M(t_{j+1}, t_j) = \exp\left(-\frac{t_{j+1} - t_j}{\tau}\right) = \exp\left(-\frac{d}{\tau}\right)$$

and

$$\eta_j = \int_{t_j}^{t_{j+1}} \exp\left(-\frac{t_{j+1} - s}{\tau}\right)\omega(s)\,ds$$

Note that $M(t_{j+1}, t_j)$ is actually independent of time: it will be noted m from now on. The variance $\sigma_p^2(t_j)$ of the Gauss–Markov process satisfies the propagation equation

$$\sigma_p^2(t_{j+1}) = m^2\sigma_p^2(t_j) + Q$$

Assuming that the covariance Q is independent of time and that the process has been operating for a long time, a steady state is reached and

$$Q = (1 - m^2)\sigma_p^2$$

The steady-state standard deviation σ_p is the noise level reached by the stochastic process after a time that is long compared with the correlation time.

So far we have only considered the propagation of the stochastic parameters. However, the time update must also include the mapping of the spacecraft orbital state from one batch to the next. The complete state vector is

$$\chi(t) = \begin{bmatrix} x(t) \\ p(t) \\ y \end{bmatrix}$$

where $x(t)$ is the satellite orbital state (usually, three positions and three velocities), $p(t)$ is the vector of stochastic parameters, and y is a vector of bias parameters.

The propagation equation for the complete state from batch j to batch $(j+1)$ is

$$\begin{bmatrix} x \\ p \\ y \end{bmatrix}_{j+1} = \begin{bmatrix} \phi_x & \phi_{xp} & \phi_{xy} \\ 0 & m & 0 \\ 0 & 0 & I \end{bmatrix} \begin{bmatrix} x \\ p \\ y \end{bmatrix}_j + \begin{bmatrix} 0 \\ \eta_j \\ 0 \end{bmatrix}$$

where $\phi_x(t_{j+1}, t_j)$, $\phi_{xp}(t_{j+1}, t_j)$, and $\phi_{xy}(t_{j+1}, t_j)$ are transition matrices computed from the partial derivatives resulting from the integration of the variational equations. For practical reasons, the pseudo-epoch orbital state[4,5]

$$X_j = \phi_x(t_0, t_j)[x(t_j) - \phi_{xy}(t_j, t_0)y]$$

is used instead of the current state to ease computations. This also ensures compatibility with the standard orbit determination filter, as the pseudo-epoch state is equivalent to a set of initial conditions at epoch time. The actual complete state is therefore

$$\Xi(t) = \begin{bmatrix} X(t) \\ p(t) \\ y \end{bmatrix}$$

Once the equations for the propagation of the state vector are established, the next step is to process data. If we note the square root information array corresponding to the a priori information available at time t by $[\tilde{R} : \tilde{z}]$, all information gathered before t can be summarized in the equation

$$\tilde{z} = \tilde{R}\Xi + \tilde{\theta}$$

where $\tilde{R}$ is an upper triangular matrix that is the inverse of the square root of the covariance.

For the measurement taken at time t, the residual z, that is, the difference between the observed and the computed value, can be expressed as

$$z = A\Xi + \theta$$

where A is the matrix of measurement partials and θ is a zero mean white noise vector.

The combined a priori and measurement equations

$$\begin{bmatrix} \tilde{R} \\ A \end{bmatrix} \Xi = \begin{bmatrix} \tilde{z} \\ z \end{bmatrix} - \begin{bmatrix} \tilde{\theta} \\ \theta \end{bmatrix}$$

are reduced thanks to a Givens transformation to

$$\begin{bmatrix} \hat{R} \\ 0 \end{bmatrix} \Xi = \begin{bmatrix} \hat{z} \\ e \end{bmatrix} - \begin{bmatrix} \hat{\theta} \\ \theta_e \end{bmatrix}$$

The updated square root information array $[\hat{R} : \hat{z}]$ can then be used as a priori to process the next measurement.

Once all of the measurements from batch j have been processed, the time propagation of the state vector is taken into account as one more measurement equation. This provides the a priori information array for batch $j+1$. This process continues until t_{end} is reached. The values of the orbital state and biases are then computed by solving the least-square problem

$$\hat{\Xi} = \hat{R}^{-1}\hat{z}$$

A smoother is then applied to recover the values of the stochastic parameters. Evolution equations for the state are backward propagated in the same way as in the filter. At the same time, the white noise nature of $\omega(t)$ is verified.

Orbit Determination Configuration

The orbit determination configuration is dictated by two constraints.

1) We do not know how to iterate with stochastic parameters. After the first iteration, a realization of the stochastic process is obtained. At the second iteration, the solved-for parameters are corrections to the results of the first iteration to obtain a stochastic parameter with the given characteristics. The increment, however, is not a Gauss–Markov process, and so far we do not know how to characterize it.

2) We cannot solve for per pass parameters while processing data in batches because of practical conflicts between the two ways of distributing data among batches.

As a consequence, we do not iterate solutions, and we use values for frequency and troposphere biases coming from a preliminary precise orbit determination. Precise orbits are computed for all spacecraft equipped with DORIS by the Service d'Orbitographie DORIS (SOD) using the ZOOM software.[6] For TOPEX/Poseidon, both DORIS only and DORIS with SLR orbits are computed. These orbits serve as dynamical references for the reduced dynamics solutions. Their accuracy is typically on the order of 5- and 10-cm rms in the radial direction for TOPEX/Poseidon and SPOT, respectively, and so it is legitimate not to iterate.

The amplitudes of the once per revolution empirical corrections, as well as the values of the 12-h drag coefficients (6 h in the case of SPOT), and the zenith troposphere delays come from the precise orbit solution. The frequency biases come from a solution using Guier formalism. All of these parameters are held fixed in the stochastic solution, although only the initial conditions and the stochastic force are solved for.

The resulting reduced dynamics orbits are truncated at both ends to suppress periods during which the stochastic parameters could not be properly determined because of the lack of data in neighboring batches. A segment of three times the correlation time, that is, 75 min, is removed at both ends.

Tuning of the Stochastic Parameters

The stochastic parameters are characterized by three quantities: the batch duration d, the correlation time τ, and the steady-state standard deviation σ_p. All three have to be chosen by the user. However, there is no strategy for finding the best set of values. In practice, the selected values correspond to an optimum reached through trial and error.

Ideally the batch duration and the correlation time should be as small as possible to best follow the short period fluctuations of the

unmodeled forces. The orbital coverage provided by the DORIS beacon network is not perfect, and there are periods during which no measurements are taken. Beacon failures, industrial interference, or receiver problems tend to create even larger periods without data. During these periods, it is impossible to determine any corrections to the model.

An empirical study was conducted to determine the minimum values of the batch duration and the correlation time. Good results were obtained with values of d ranging from 300 to 500 s. Both endpoint values lead to nearly identical results, with very little difference in computer time requirement, and so the value 300 s was selected.

The correlation time has to be carefully chosen, as this is the parameter that will make it possible for the filter to handle periods with little or no data. With a batch duration fixed at 300 s, an optimal choice for the correlation time is 1500 s. On the one hand, if τ is less than 1500 s, the filter does not carry enough information from the last batch to the current batch, and the values of the stochastic parameters blow up whenever there are too few data points. On the other hand, if τ is more than 1500 s, some information is lost because the stochastic parameters cannot follow the rapid fluctuations of the unmodeled forces. Note that the value 1500 s is already fairly large: it is about one-fourth of the orbital period.

The value of σ_p is selected by comparing solutions obtained with a wide range of values. A value of σ_p equal to 2×10^{-8} m/s^2 leads to consistent results across a few cycles. For this value the amplitude of the stochastic force is at the level of 10^{-9} m/s^2 and its behavior is entirely acceptable (see the following paragraph). When the value of σ_p is larger (such as 2×10^{-7} or 2×10^{-6}), the stochastic force absorbs nondynamical problems (e.g., local problems as a result of incorrect station coordinates).

Behavior of the Stochastic Force

Figure 1 presents the amplitude of the stochastic force for TOPEX/Poseidon's cycle 43. The magnitude of the stochastic force is 10^{-9} m/s^2 in the three directions. The along-track component is the largest, as should be expected. This component absorbs the unmodeled part of the atmospheric drag, among other things. The overall behavior of the force is relatively smooth, and there is no clearly visible period.

The overall level of this force is compatible with the quoted accuracy[7] of DORIS, of about 10^{-10} m/s^2 for daily averages, which corresponds to an accuracy better than 2×10^{-9} m/s^2 per 5-min batch.

The periodogram of the along-track component, shown in Fig. 2, exhibits the $1/f$ behavior characteristic of the first-order Gauss–Markov process.

The peaks at 6.5 rad/day (log 6.5 = 0.81 in Fig. 2) and 82 rad/day (log 82 = 1.91 in Fig. 2) correspond, respectively, to 1/day and 1/revolution. The stochastic force thus absorbs the once per day and once per revolution residual component not removed by the 12-h drag coefficient and the empirical 1/rev factor. A comparison of periodograms of DORIS and SLR residuals computed with the reference and the corrected orbits shows that the signals at these two frequencies disappear with the corrected orbit.

Figure 3 shows the Allan variance[8] of the along-track component of the stochastic force. For small values of dt, the slope of the Allan variance is close to 1, which is characteristic of a random walk process. Around dt equal to 3000 s (i.e., twice the correlation time τ), the slope changes and, for large values of dt, takes a value of -1 characteristic of white noise.

When σ_p is larger than 2×10^{-8} m/s^2, such as 2×10^{-6} m/s^2, the behavior of the stochastic force is completely perturbed. The amplitude goes up to about 10^{-7} m/s^2 and the periodogram is nearly flat, with a large peak at 2/revolution. And the orbit is significantly degraded. All of the results of orbit quality tests with the orbit computed with σ_p larger than 2×10^{-8} m/s^2 are worse than the results obtained with the orbit computed with σ_p equal to this value. The 2/revolution signature has been identified in the Centre National d'Etudes Spatiales (CNES) DORIS residuals for quite some time. Recent works show that the origin of this signal is the incorrect match between the station coordinate set and the Earth orientation parameters. This signal disappears from the DORIS residuals when the new set of station coordinates computed by the SOD is used. However, in this paper we only consider solutions where σ_p is equal to 2×10^{-8} m/s^2 and where this station coordinate effect is without influence.

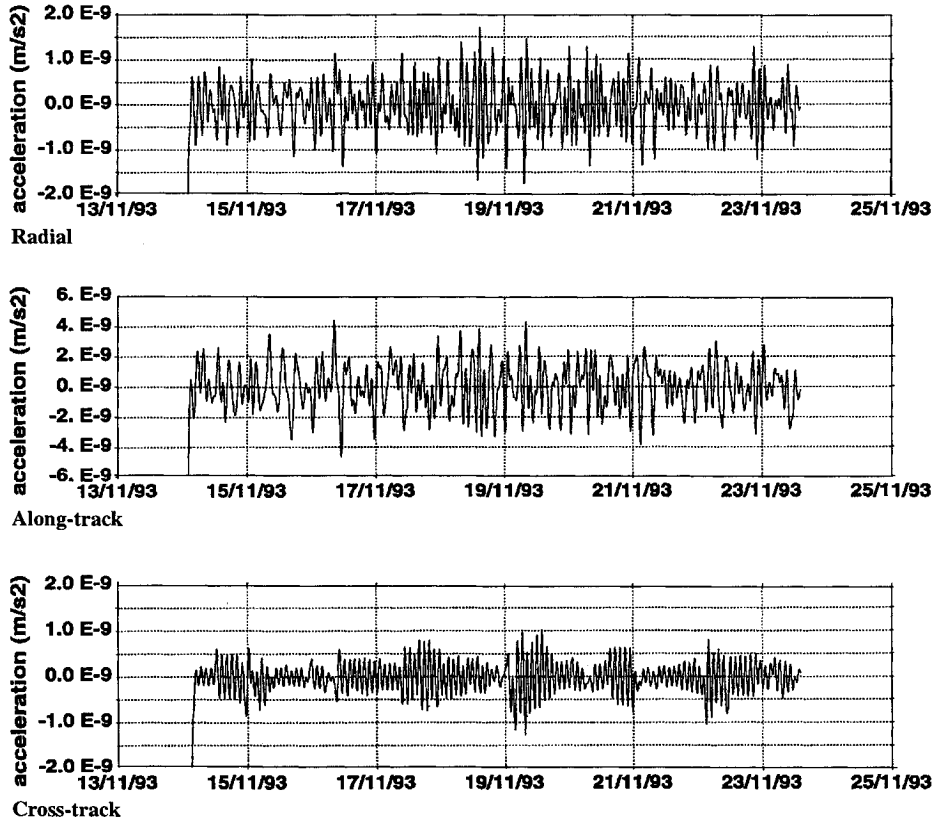

Fig. 1 TOPEX/Poseidon cycle 43 stochastic force.

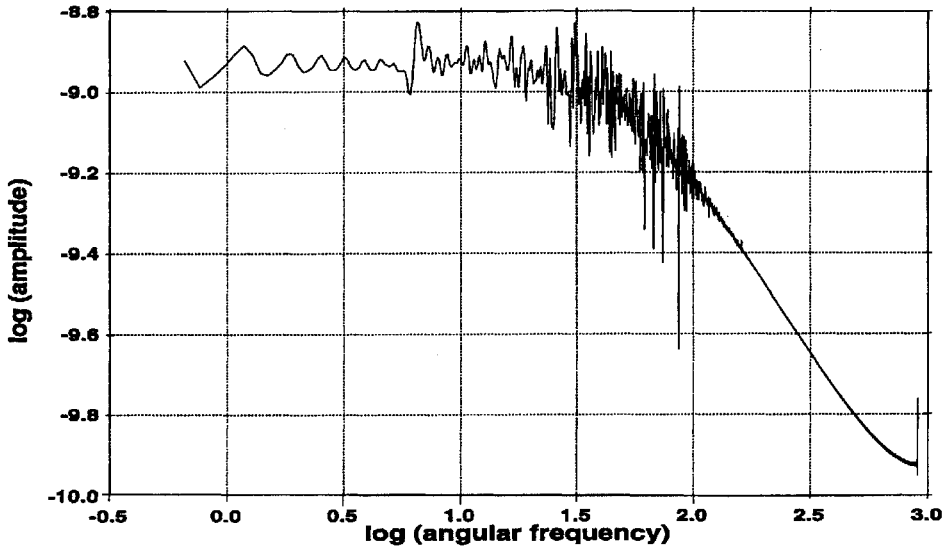

Fig. 2 Periodogram of the along-track component of the stochastic force.

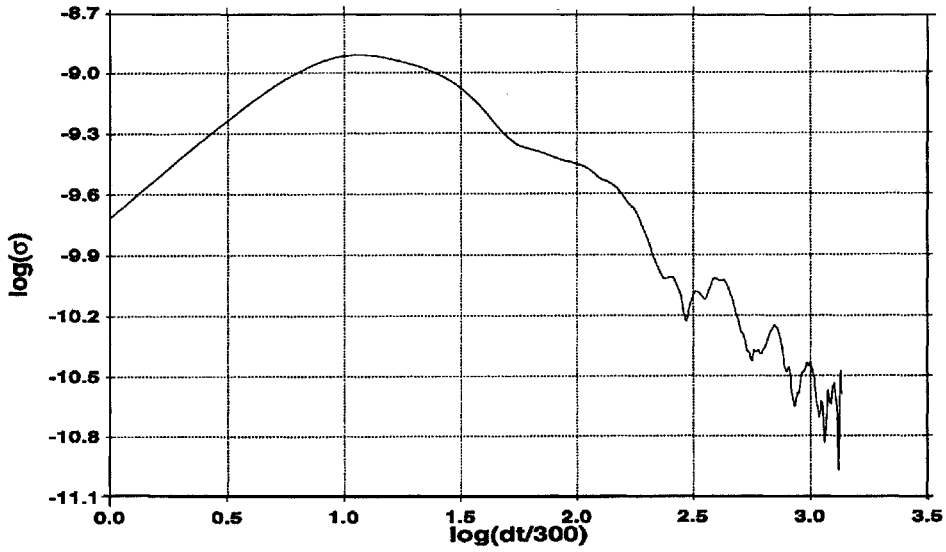

Fig. 3 Allan variance of the along-track component of the stochastic force.

Results with TOPEX/Poseidon

In this section and the following, we denote the reference orbit computed with the standard method by A and the orbit obtained with the stochastic solution (our reduced dynamics orbit) by B. Except when explicitly indicated, A and B orbits are computed using both DORIS and SLR data.

Fits to the tracking data are usually a good indication of orbit quality. Table 1 gives the values of the rms of the DORIS and SLR residuals computed with the A and B orbits. So many parameters are adjusted in the fit that the decrease in the residuals is not very significant. However, the fact that the improvement is much better for the SLR data than for DORIS data is instructive. Most of the power in the DORIS residuals lies in the strong signal at 2/revolution. As the stochastic solution is prevented from absorbing this nondynamical signature, it cannot significantly reduce the DORIS residuals.

A more meaningful test of the orbit quality is provided by the results of Table 2. In this test, orbits are produced using DORIS data only. The results show that the SLR residuals are lower with the B orbits than with the A orbits, which means that the B orbits are better than the A orbits. The comparison of both orbits with the solution obtained with DORIS and SLR data shows that the improvement brought by the reduced dynamics is mostly in the cross-track direction. It is suspected that the CNES orbits are weak in the cross-track direction because of the ocean tide model that is used.

Comparison of altimeter crossover data, which are not used in the orbit computation, provides another estimate of the orbit quality improvement brought by the reduced dynamics approach. Table 3 lists unedited altimeter crossover statistics. The results show a small but systematic reduction in residual level.

Orbit overlaps are usually good tests of orbit quality. Results given in Table 4 correspond to a 1-day overlap between 4-day arcs. The improvements brought by the stochastic corrections are impressive; however, they are not a sign of orbit quality. It is a characteristic of the stochastic method to adapt the orbit to follow the measurements. During the overlap period, both orbits are thus corrected in a similar way to best fit the measurements. The reduced dynamics orbit is weakly correlated over periods longer than three times the correlation time, and so it is natural that the influence of the three days of data before and after is not felt during the day in common. Comparison of the stochastic forces over this common period shows that both solutions are very close.

Similarly, endpoint overlaps are poor tests of orbit quality for reduced dynamics solutions. Because of the truncation at both ends, the orbits must have more than three correlation times of data in common to have common periods. And this is enough time for the stochastic orbits to converge toward a unique solution.

Intercomparisons with orbits produced by the NASA Goddard Space Flight Center (GSFC) and JPL provide some more information on the error level of the orbits under study.

Orbits are produced by GSFC using a different reference frame, different station locations, and different nonconservative force models from ours. In addition, they adjust an along-track constant acceleration per day and along-track and cross-track 1/revolution coefficients per day. In contrast, we adjust a 12-h drag coefficient and along-track and cross-track 1/revolution terms per period of three to four days.

The computation of the JPL dynamical orbits differs from our computation by the force models and the data type used. Moreover, they process their data in 30-h batches and adjust constant, 1/revolution, and 2/revolution empirical parameters. They also solve for Earth orientation parameters.

Table 5 lists the rms difference between our orbits and those of GSFC. Overall, B orbits are farther away from the GSFC orbits than A orbits, except in the cross-track direction. This confirms the previously mentioned result regarding cross-track improvement. The radial difference is not significant. It has also been established that part of the radial bias is removed when dynamical relativistic corrections are applied.

Table 6 lists the rms difference between our orbits and JPL's dynamical orbits, and Table 7 lists the rms difference between our orbits and JPL's reduced dynamics orbits. There is no clear trend in the results. In particular, the two reduced dynamics orbits are not any closer to each other than the dynamical orbits. This is not a negative point because the TOPEX/Poseidon precise orbit determination groups work in collaboration to obtain more accurate models. As a result they develop similar orbit determination configurations and obtain very close dynamical orbits. This kind of work does not exist with the reduced dynamics orbits.

The comparison of the GPS dynamical orbits with our dynamical orbits shows a daily along-track signal. The amplitude of this periodical term increases to about 20 cm when the GPS reduced dynamics orbits are compared with our dynamical orbits (Fig. 4).

Table 1 DORIS and SLR residuals

RMS	DORIS, mm/s	SLR, cm
CY041 A	0.88	5.5
B	0.81	3.5
CY043 A	0.89	7.1
B	0.80	4.1
CY049 A	0.83	5.8
B	0.78	4.0
CY063 A	0.81	3.6
B	0.79	2.9

Table 2 DORIS and SLR residuals for a DORIS only solution

RMS	DORIS, mm/s	SLR, cm
CY041 A	0.88	8.5
B	0.81	7.2
CY043 A	0.87	11.1
B	0.79	8.8

Table 3 Altimeter crossover residuals

Crossovers	Mean, cm	RMS, cm
CY041 A	−2.9	12.63
B	−2.5	12.63
CY043 A	−1.4	12.70
B	−0.8	12.33
CY049 A	0.6	11.07
B	0.7	10.85

Table 4 Orbit overlap

RMS, cm	Radial	Along-track	Cross-track
CY043 A	2.6	21.0	3.7
B	0.6	1.6	3.3

Table 5 Comparison with GSFC orbits

Mean/rms	Radial, cm	Along-track, cm	Cross-track, cm
CY041 A	−0.74/2.8	−5.6/13.0	−0.01/3.0
B	−0.76/3.5	−4.5/15.1	0.00/2.8
CY043 A	−0.92/2.6	−5.2/10.6	0.03/5.1
B	−0.89/3.1	−3.6/13.8	0.04/4.8
CY049 A	−0.90/2.0	−2.9/6.5	−0.20/3.9
B	−0.91/2.3	−2.3/10.1	−0.19/3.2
CY063 A	−0.81/1.8	2.5/7.6	0.32/3.4
B	−0.81/2.1	2.5/9.3	0.32/3.4

Table 6 Comparison with JPL dynamical orbits

Mean/rms	Radial, cm	Along-track, cm	Cross-track, cm
CY041 A	−0.35/2.1	−0.4/10.8	0.9/5.9
B	−0.36/2.5	−0.6/8.2	0.9/6.1
CY043 A	−0.42/2.0	1.5/11.6	−4.1/8.5
B	−0.40/2.3	3.0/11.7	−4.1/8.2
CY049 A	−0.65/2.0	−0.6/8.3	1.1/7.3
B	−0.66/2.4	0.1/9.6	1.1/7.0

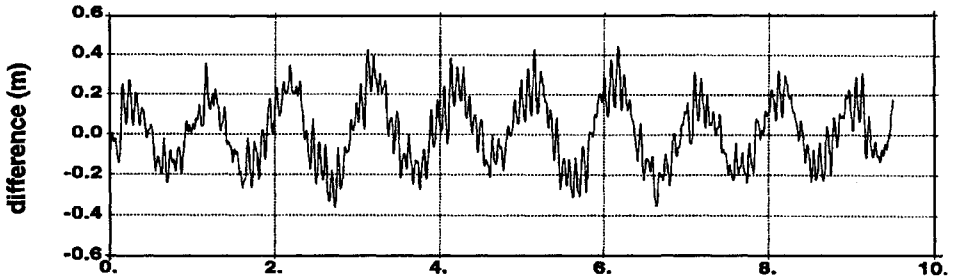

Comparison of CNES dynamical orbit with JPL reduced dynamics orbit

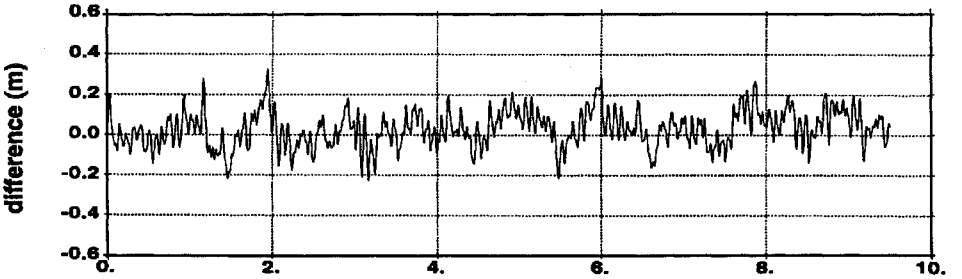

Comparison of CNES reduced dynamics orbit with JPL reduced dynamics orbit

Fig. 4 Orbit differences in the along-track direction.

This signal is strongly attenuated when our reduced dynamics orbits are compared with both sets of GPS orbits. The origin of this signal is unknown. JPL solves for polar motion, whereas we use the International Earth Rotation Service published values: this difference could introduce such a daily term. However, the fact that it disappears when we introduce the stochastic force indicates that there is an actual physical effect that is not properly modeled in the standard solutions.

To best study the geographical correlation of radial differences between the dynamical and reduced dynamics solutions, we display these corrections as a function of longitude and latitude on a map. Separate maps are created for descending and ascending orbits. On both kinds of maps, the largest corrections occur over the same areas for all of the cycles. The radial corrections are thus geographically correlated. In addition, the largest radial corrections occur over the same areas where the differences between JPL's dynamical and reduced dynamics orbits are maximum. Our radial corrections are significantly smaller than those of JPL. However, this comparison is not very meaningful as we do not use reference orbits of similar accuracy.

Results with SPOT

SPOT 2 and SPOT 3 are two French Earth observation satellites equipped with DORIS receivers. Accurate orbits for both of these spacecraft are computed on a routine basis. It is therefore natural to try to improve the orbit quality through the use of the reduced dynamics approach. Unfortunately, as DORIS is the only tracking system, it is difficult to really assess the impact of the method. However, as both SPOT 2 and SPOT 3 are on the same orbit, it is possible to compare the stochastic force measured by each satellite. The drag force depends on latitude and on local time and weakly on longitude. SPOT 2 follows SPOT 3 with a 43-min time lag. Thus, SPOT 2 is over a point with the same latitude and same local time as SPOT 3 was 43 min before. Only the longitude changed. Atmospheric density models exhibit very little dependency on the longitude, and so the drag force of SPOT 2 must be correlated with that of SPOT 3 with a time difference of 43 min. However, as the longitude changes, SPOT 2 is not over the same point as SPOT 3 was 43 min before. Geographically correlated forces will therefore not be correlated. This should help identify the origin of the corrections.

Our analysis has been performed on a 7-day arc with good coverage for both SPOT 2 and SPOT 3. Reference orbits are computed for SPOT as for TOPEX/Poseidon, except that the GRIM4-C4P gravity field is used instead of JGM-2 and 6-h drag coefficients are used instead of 12-h coefficients. Reduced dynamics orbits are obtained in the exact same manner as for TOPEX/Poseidon.

Table 8 lists the rms of the DORIS residuals for both SPOT 2 and SPOT 3. As mentioned earlier, there is no significant improvement of the residual level. Here again, most of the residual power is at the 2/revolution period, and this signal is barely attenuated in the stochastic solution.

The amplitude of the stochastic force is about 10^{-9} m/s^2 in the three directions. Figure 5 displays the along-track component for both SPOT 2 and SPOT 3. The temporal variations of both forces show some similarities, but they are overall very different. A recent study has shown that the drag coefficients of SPOT 2 and the drag coefficients of SPOT 3 are correlated with a time lag of 43 min.[9] As the major part of atmospheric drag is absorbed by the drag force model, the residual part absorbed by the stochastic force is not high enough to exhibit a strong correlation. Hence, the noncorrelation of the forces acting on SPOT 2 and SPOT 3 indicates that the stochastic force is mostly of geographically correlated origin. However, since the launch of SPOT 3, solar activity has been rather low. These results might be different in the presence of high solar activity.

Table 7 Comparison with JPL reduced dynamics orbits

Mean/rms	Radial, cm	Along-track, cm	Cross-track, cm
CY041 A	−0.44/2.7	−0.6/12.4	1.0/6.7
B	−0.45/2.7	−0.7/7.8	1.0/6.8
CY043 A	−0.56/3.3	1.6/16.2	−4.1/9.1
B	−0.53/2.6	3.1/9.5	−4.0/8.8
CY049 A	−0.56/2.9	0.0/10.6	1.1/7.9
B	−0.57/2.6	0.6/8.2	1.2/7.6

Table 8 DORIS residuals

RMS	DORIS, cm/s
SPOT 2 A	0.12
Arc 88 B	0.11
SPOT 3 A	0.11
Arc 19 B	0.10

Conclusion

The results obtained so far are very encouraging. They prove that a stochastic force with a time resolution of 5 min can effectively be determined from the DORIS and SLR data. In addition,

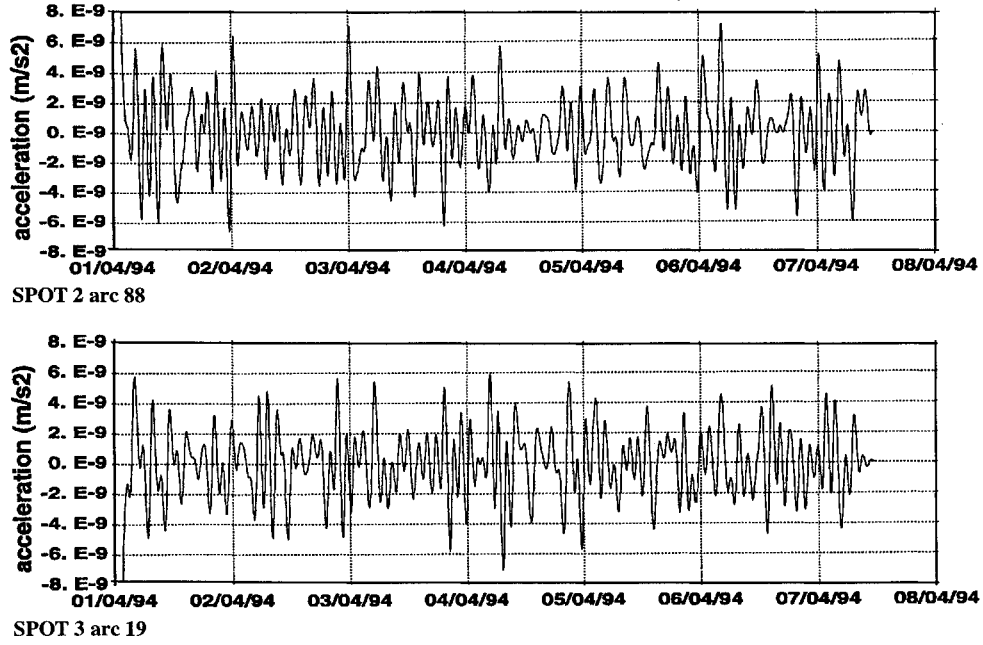

Fig. 5 Along-track component of the stochastic force.

several tests indicate that our TOPEX/Poseidon reduced dynamics orbits are more accurate than the standard dynamical solutions. However, these are only preliminary results. More cycles of data will need to be processed to properly evaluate the advantages of this method.

The comparisons of our reduced dynamics orbits with orbits from other groups lead to disconcerting results. These issues need to be further investigated. Our orbits do exhibit a significant geographical correlation of the radial orbit correction. This correlation is also one of the major characteristics of the GPS reduced dynamics orbits.

The existence of a twice per revolution signal in the CNES DORIS residuals limits our ability to apply the stochastic approach to SPOT. Nevertheless, we are confident that our method can significantly contribute to improving the orbit quality for spacecraft such as SPOT or ENVISAT for which uncertainties in the atmospheric drag models play an essential role.

Acknowledgments

The first author was supported by a grant from both the Centre National d'Etudes Spatiales and the Service Technique de la Navigation Aérienne, Délégation Générale de l'Aviation Civile. The authors wish to thank their Jet Propulsion Laboratory colleagues for providing them with TOPEX/Poseidon orbits.

References

[1]Mohan, S. N., Bierman, G. J., Hamata, N. E., and Stavert, R. L., "Seasat Orbit Refinement for Altimetry Application," *Journal of the Astronautical Sciences*, Vol. 28, No. 4, 1980, pp. 405–417.

[2]Bertiger, W. I., et al., "GPS Precise Tracking of TOPEX/POSEIDON: Results and Implications," *Journal of Geophysical Research*, Vol. 99, No. C12, 1994, pp. 24,449–24,464.

[3]Tapley, B. D., et al., "Precision Orbit Determination for TOPEX/POSEIDON," *Journal of Geophysical Research*, Vol. 99, No. C12, 1994, pp. 24,383–24,404.

[4]Bierman, G. J., *Factorization Methods for Discrete Sequential Estimation*, Academic, New York, 1977.

[5]Lichten, S. M., "Estimation and Filtering for High-Precision GPS Positioning Applications," *Manuscripta Geodetica*, Vol. 15, No. 3, 1990, pp. 159–176.

[6]Nouël, F., et al., "Precise CNES Orbits for TOPEX/POSEIDON: Is Reaching 2 cm Still a Challenge?" *Journal of Geophysical Research*, Vol. 99, No. C12, 1994, pp. 24,405–24,419.

[7]Tapley, B. D., "Precision Orbit Determination Studies for TOPEX/Poseidon Follow On," TOPEX/Poseidon Science Working Team Meeting, Status Rept., Toulouse, France, Dec. 1993.

[8]Walls, F. L., and Allan, D. W., "Measurements of Frequency Stability," *Proceedings of the IEEE*, Vol. 74, No. 1, 1986, pp. 162–168.

[9]Goselink, A. H. J., "The Correlation of the Drag Coefficients of SPOT2 and SPOT3," Practical Training Rept., Faculty of Aerospace Engineering, Delft Univ. of Technology, Delft, The Netherlands, April 1995.